Experimental research on microscopic displacement mechanism of CO_2-water alternative flooding in low permeability reservoir

Hongyan Han[1], Weiyao Zhu[1,3], Yunqian Long[2], Hongqing Song[1] and Kun Huang[1]

[1] School of Civil & Recource Engineering, University of Science and Technology Beijing, Beijing 100083, China;
[2] Innovation Application Institute, Zhejiang Ocean University, Zhoushan 316022, China.

[3] weiyaook@sina.com

Abstract. This paper provides an experimental method to deal with the problems of low oil recovery ratio faced with water flooding utilizing the CO_2/water alternate displacement technology. A series of CO_2/water alternate flooding experiments were carried out under 60℃ and 18.4MPa using high temperature / pressure microscopic visualization simulation system. Then, we used the image processing technique and software to analyze the proportion of remaining oil in the displacement process. The results show that CO_2 can extract the lighter chemical components in the crude oil and make it easier to form miscible phase, which can reduce the viscosity and favorable mobility ratio of oil. What's more, the displacement reduces the impact of gas channeling, which can achieve an enlarged sweeping efficiency to improve filtration ability. In addition, the CO_2 dissolved in oil and water can greatly reduce the interfacial tension, which can increase the oil displacement efficiency in a large extent. Generally speaking, the recovery rate of residual oil in the micro - model can be elevated up to 15.89% ~ 16.48% under formation condition by alternate displacement.

1. Introduction

The Low permeability fractured reservoir is characterized by complex network of fracture and rapid production decline rate; furthermore, it remains a worldwide problem as to how to undertake effective energy supplement procedure [1]. To achieve a better development outcome, three basic technical requirements need to be taken into consideration: a better performance in injectivity, a promising recovery rate as well as an effective utilization of artificial energy supplement. Gas flooding, particularly CO_2 flooding, serves as a potential approach to improve the injectivity and displacement efficiency to a large scale. CO_2 flooding practice has been proved effective from at home and abroad due to its potential to enter the tiny pores [2]. Besides, with multiple reaction mechanisms taking place during displacement, it facilitates the exploitation of crude oil. As a result, it normally witnesses a 6~15% increase in the recovery rate than that of regular water flooding.

The water alternate gas (WAG) WAG process consists of water and gas being alternately injected. One of the objectives of CO_2 WAG is to reduce the oil viscosity by injecting CO_2 slug, and and improve mobility ratio (MR), and then displacing the less viscous oil with water [3-5]. Also, the gas helps displacing the oil that has not been displaced by the water by creating a more efficient sweep. However, most of the crude oil reservoirs in Zhongyuan Oil Field of China have relatively low

Content from this work may be used under the terms of the Creative Commons Attribution 3.0 licence. Any further distribution of this work must maintain attribution to the author(s) and the title of the work, journal citation and DOI.
Published under licence by IOP Publishing Ltd

reservoir pressure so miscibility between the oil and CO_2 cannot normally be achieved. Also, water flooding result in creating low-resistance channels. CO_2-WAG reduces the detrimental effects of fingering because the injected CO_2 tends to occupy (a) some of the low-resistance channels created by water and (b) some of the pores to reduce the relative permeability to water [6-8].

Physical simulation is an important method to obtain clear mechanism and accurate parameters on displacing oil techniques. As one of physical simulation methods, microscope infiltrating fluid simulation can provide visualization and semi-quantitative data. Most experiments on CO_2-WAG oil are under high pressure in a range of temperatures and depths in which it is hard to observe the movement of oil and water and the distribution of oil, water and gas. This paper builds a visual microscope infiltrating fluid simulation under high temperature and high pressure（≤25MPa、≤ 110°C）. We measure the pulling force and viscosity between CO_2 and oil which depicts the CO_2-WAG displacing oil mechanism. We compare the effects of CO_2-WAG oil under high pressure/temperature and that under high pressure but normal temperature. Result shows that CO_2-WAG displacing oil under high pressure/temperature avoids the shortage of gas breakthrough that this technique under normal temperature suffers. And it can increase the fluidity of remaining oil, so as to improve the efficiency of oil displacing.

2. Experimental section

2.1. Materials preparation

The visual model is made of a two-dimensional pore structure etched onto the surface of a flat glass plate, and the pore structure is identical with the realistic cross-section image of a sandstone core from the Pujian 4-42 of Zhongyuan Oil Field. The whole experiment uses photochemical etching process. Pore structure is etched to optical glass precisely after appropriate microscope amplification. Then the glass is coated with light-sensitive material for exposure with hydrofluoric acid, finally finished the model through high heat sintering. Model has oil-wetted surface and the flow network structure exists heterogeneity, has the property of reservoir rock pore system real standard and similar geometry and shape geometry and shape distribution characteristics. The external size and pore volume of the model are 40 mm × 40 mm and 50 μL, channel section for elliptic, and visibility. The photograph of the micro-model used in this study is shown in Figuer.1(a). There are two etcher inlet/outlet ports at opposite corners of the pore network, simulating the injection well and production well.

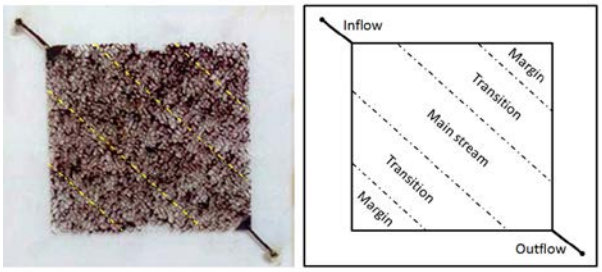


Figure 1. The visual microscopic model and region division of the model.

The properties of the oil is viscosity 64.8 mPa·s, density 0.74～0.75 g/cm^3 ; The properties of the water is viscosity 0.5mPa·s, mineralization 23.7×10^4 mg/L and concentration Cl^- 16×10^4 mg/L. Temperature 60°C, pressure 18.4 MPa, CO_2 (99.9%).

2.2. Experimental and analysis

2.2.1. Microscopic flooding experiment. The two-dimensional microscopic flooding apparatus is shown schematically in Figure. 2. The experimental setup is composed of two main systems, the flooding system and image capturing systems with some accessories. The heart of the apparatus is the micro model. It was covered by another glass plate to create an enclosed pore space. The photograph of the micro model used in this study is shown in Figure.1(a). In the steel model holder (a hollow

cylinder), the micro model is clamped horizontally by thick glasses and filled with water to load the overpressure, allowing light to penetrate through vertically. This special holder and a back-pressure valve are used to mimic the high pressure in oil reservoirs, and the accumulators are used for holding and injecting the liquids (crude oil, brine and CO_2).

The procedure for microscopic flooding experiments is similar to that of core flooding experiments process. After the water saturation, oil saturation and water flooding stages, we continue to inject CO_2-water-CO_2 alternately and every injection is 0.2PV. Finally, the experiment followed by water flooding. After that, the micro-model was cleaned by circulating petroleum ether and distilled water. The rates of all injections in the microscopic flooding experiments were 0.05 ml/min (the capillary number of water-flooding, 5.3×10^{-6}). During the process, the micro-model was kept at 60°C and 18.4 MPa (miscible) of overpressure. The morphology of remaining oil was captured constantly. The color of the produced liquid was observed during the whole process of the experiment, and then the chemical composition was analyzed using gas chromatography. Oil saturation determination from images is difficult and time consuming. To tackle this issue, the original images were sharpened to improve the contrast, and then analyzed with a program developed using MATLAB. The oil saturation was calculated by the area proportion of oil to pore space.

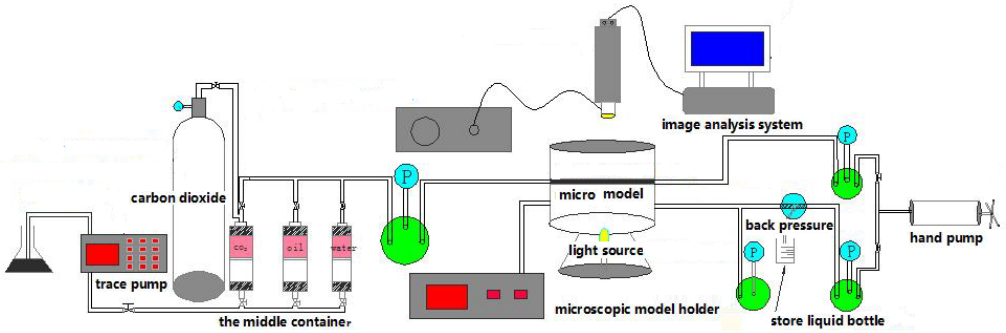


Figure 2. High temperature and high pressure co_2/water micro displacement device.

2.2.2. Partition of the sweep area. To demonstrate the sweep efficiency during flooding, the micromodel was divided into three specific regions along the normal of the major flooding trajectory to individually measure the oil saturations (Figure 1b). The three regions, including the main stream, the transitions, and the margins, occupied 39.39, 40.84, and 19.76% area of the total model, respectively. In the three regions, eight, eight, and four images of different sites were recorded, respectively. The oil saturation of each region was reported as the arithmetic average of the oil saturations of all recorded sites in the region. In terms of the total model, the oil saturation was the average of the three regions weighted by their area proportions.

2.2.3. Viscosity measurement and Interfacial tension measurement. The viscosity was measured at 60°C pour a certain amount of mixture of CO_2 and oil under different pressures. Change temperature, and when temperature is stable, we measure its viscosity under different pressures. In order to guarantee reliability and repeatability, each measurement was performed four times; The interfacial tensions was measured at 60°C between the crude oil and the CO_2, using the interfacial tension of high temperature and high pressure measuring device. In order to guarantee reliability and repeatability, each measurement was performed four times.

3. Results and discussions

3.1. Viscosity analysis

By measuring the viscosity of the mixture of oil, water and CO_2 (Gas oil ratio Rs=6,15,25,35,45,55） under different temperatures and pressures, we get the viscosity/temperature curve under different pressures as Figure 3

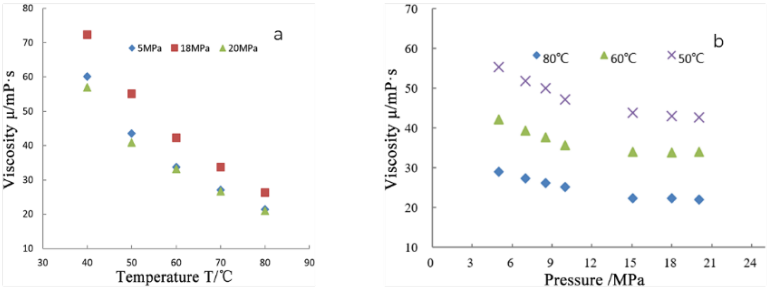


Figure 3. a The viscosity - temperature characteristic curve of oil and gas mixture;
b The mixture of oil and gas viscosity and pressure curve under different temperature.

From Figure 3a, we can infer that under all pressures the viscosity of oil decreases exponentially as the temperature increases. Mixed with CO_2, viscosity of oil decreases a lot. Under all pressures, the viscosity of oil decreases nearly exponentially as the temperature increases. This is similar to pure oil. When oil is mixed with CO_2, its density decreases, intermolecular interaction gets weaker which leads to low viscosity. Viscosity is sensitive to temperature. When temperature increases, intermolecular interaction in oil gets weaker and viscosity decreases. From Figure 3b, we can see that the viscosity of the mixture of CO_2 and oil decreases for a period and then increase indistinctly as the pressure increases. This phenomenon is because in the mixture of oil and CO_2, when the pressure is lower than saturation pressure, more CO_2 is mixed into oil as pressure increases which decrease the viscosity. when the pressure is higher than saturation pressure, no more CO_2 will be mixed into oil, the mixture contrasts as pressure increases, and this makes its density increase, molecular spacing decreases, inner friction increases and viscosity rises. When the pressure is equal to saturation pressure, the CO_2 in oil reaches its maximal, the composition of the mixture reaches the best and the viscosity falls into the lowest. As the temperature and the percentage of oil rises, CO_2 is easy to be separated.

3.2. Interfacial Tension Analysis

With the increase of pressure, the interfacial tension between CO_2 and crude oil decreases gradually. As shown in Figure. 4a, the interfacial tension witnesses a rapidly growth when the pressure is lower than 18.4 MPa , by contrast, when the pressure rises above 18.4MPa, the interfacial tension decreases in a more moderate way. The increased CO_2 gas in crude oil contributes to the reduced density difference and intermolecular difference between the two phases, as a result, the imbalance of the molecular force field decreases to a large extent, thus creating a lower surface tension.

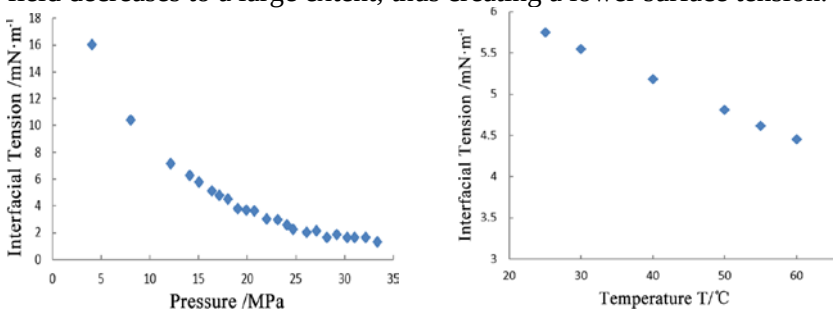


Figure 4. a Interfacial teasion between CO_2 and oil under different pressure;
b Interfacial teasion between CO_2 and oil under different temperature.

As shown in Figure. 4b, when the pressure is constant, the interfacial tension between CO_2 and crude oil decreases as the temperature rises. This is partly because the intensified molecular motion and the weakened difference in molecular force field between CO_2 and oil. The decrease in interfacial tension makes it easier to recover the residual oil adhering to the wall of the cell and those remaining in the pores. It is also noted that under the pressure of 18.4Mpa, the supercritical CO_2 is more likely to be dissolved into crude oil and water, which leads to the development of a miscible phase zone in no time as the multi-contact times increase The miscible phase zone can effectively diminish the unfavorable effect caused by the CO_2 fingering. Whereas, since the interfacial tension is not zero, it can be predicted that the miscibility is a multi-contact one.

3.3. Microscopic displacement mechanism

3.3.1. Miscible displacement mechanism. During the CO_2-WAG process, part of the injected water is forced to flow to low permeable area, which would increase the imbibition efficiency of fine pores. As results, a larger sweep area as well as a higher sweeping efficiency for per pore volume is achieved. Due to the fact that there is still some oil remaining in the throats and adhering to pore walls after flooding, besides, the injected water is inclined to flow through large pores, the displacing phase would compress the gas and opens a way to let it pass through. At the same time, a considerable portion of the gas is displaced by water in the form of dissolved gas and miscible phase.

As shown in Figure. 5, CO_2 first enters the pores along channels with less filtrational resistance. When the two phases encounter at the displacing front, a transitional zone is formed and will last for a few minutes. In addition, with the increase of CO_2 content in the transitional zone, the color of transitional zone becomes lighter accompanied by the gradual disappearance of the transitional zone. In the next stage, the transitional zone moves forward as gas is injected continuously. The miscible phase make it possible for fluid to enter those tiny pore spaces that gas barely passes, which would definitely enlarges the sweeping areas [9].

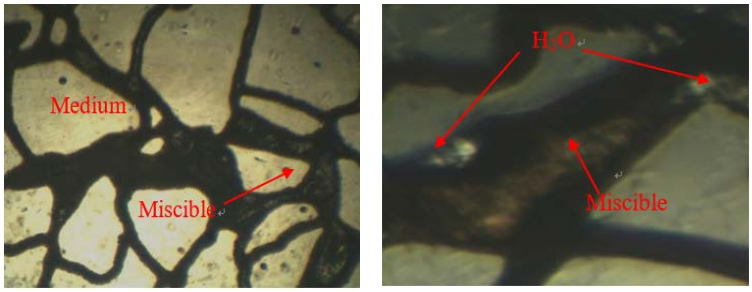


Figure 5. CO_2/ water exchange process exit flow characteristics of crude oil.

3.3.2. Extraction displacement mechanism. Since the interfacial tension of the gas-oil system is smaller than that of the gas-water system, besides, the interfacial tension of fluid tends to stay at the lowest level. As a consequence, the gas molecules are more likely to present in the remaining oil, at the same time, an increased effective size of the oil droplets containing gas phase is easily obtained. As shown in Figure. 6a and Figure. 6b, the volume of gas phase in micro-glass model gradually decreases with more dissolved of CO_2 in oil phase, which lead to the expansion of the crude oil and increase the pore volumes filled with oil phase. The method can facilitate the flow of oil in the porous medium and reduce residual oil in the model.

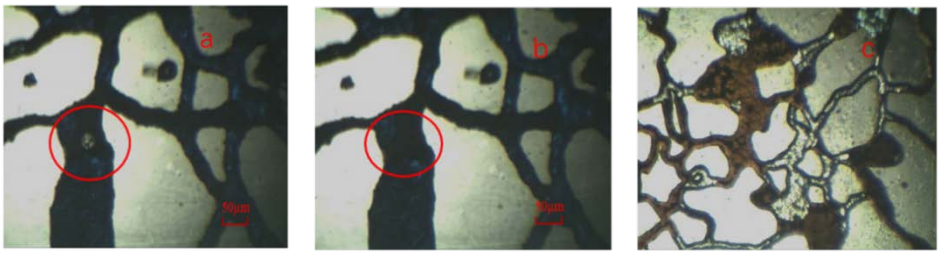


Figure 6. a and b CO_2 gas dissolution in CO_2 water alternating process
c extraction phenomenon.

CO_2 gas is likely to be dissolve in crude oil during gas and water alternate flooding process. Since CO_2 has the potential to extract some lighter or intermediate components from the crude oil, it is highly possible to obtain a miscible phase in formation. As shown in Figure. 6c, the microscopic image below shows the process of CO_2 extraction of crude oil at 18.4 MPa. It can be observed that the presence of CO_2 separates the light and heavy components from the crude oil, making it easier to extract and recover light hydrocarbon from pore spaces. In addition, chromatographic analysis shows that the chemical composition of the produced oil is quite different from than that of the original crude oil. As shown in Figure.7 The chemical composition witnessed a sharp decrease in components heavier than C_{26} and a opposite trend as to those lighter than C_{20}.

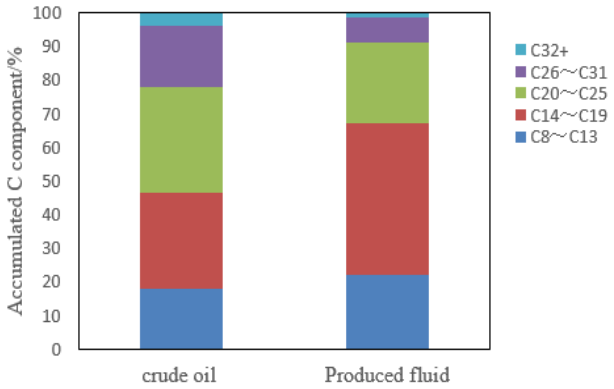


Figure 7. Variation of composition before and
after CO2/ miscible flooding.

3.3.3. Quantitative analysis of CO_2-WAG. In order to analyze the mechanism regarding CO_2-WAG process, we divided the model into three sections: main channels, transitional zone and boundary area, meanwhile, we calculated the enhanced oil recovery of each part separately. As shown in table 1, after the first water flooding, there is still 50% of oil remaining unrecovered. The saturation distribution of remaining oil can be characterized as: the main channels <transition zone <boundary area, which coincides with the fact that the injected water has a preference to main channels, leaving considerable amount of oil unrecovered in boundary areas. After finishing the CO_2-WAG flooding process, the enhanced oil recovery of crude oil in the border area and the transition zone is 32.1%and 31.2% respectively; both gained a 10% increase than that of main channels, which is 22.2%. This can be attributed to the increased sweep efficiency caused by injected CO_2, which, after oil in main channels being exploited during water flooding, gives another boost in the recovery of quite amount of oil left in border area and transitional zone.

4. Conclusions

With the increase of temperature and pressure, a favorable oil-water mobility ratio and oil displacement efficiency is achieved as a result of reduced oil viscosity and interfacial tension. Under formation condition, the occurrence of multi-contact miscibility makes it possible to achieve a higher

recovery rate during CO_2-WAG process. With the increase of CO_2 concentration, the interfacial tension of oil-water phase decreases. Accompanied by the development of regional miscible phase band, a highest recovery is observed. Furthermore, as was witnessed during experiments, miscible flooding can extract more light components from the remaining oil, thereby increasing oil recovery.

The CO_2-WAG not only avoids the occurrence of circumfluence during water flooding, but also reduces the gas channeling in high permeability formation, thus making the most use of advantages of those two methods. The quantitative analysis of images acquired from the micro-displacement process shows CO_2-WAG flooding can increase the recovery ratio up by 19.67% throughout different displacement stages.

Table 1**.** Quantitative analysis of residual oil variation in different regions of the model.

		remaining oil saturations			additional oil recovery(% OOIP)		
	region	after water flooding	CO_2 /water alternate injection	after post-water flooding	CO_2 /water alternate injection	by post-water flooding	total
Control （water flooding）	main	41.24		35			6.24
	transition	55.14		44.5			10.64
	margin	58.21		48.7			9.51
	average	51.53		42.7			8.83
WAG flooding	main	42.6	31.6	20.4	11	11.2	22.2
	transition	53.4	35.7	22.2	17.7	13.5	31.2
	margin	57.5	38.1	25.4	19.4	12.7	32.1
	average	51.37	35.13	22.67	16.24	12.47	28.5

Acknowledgment
We gratefully acknowledge the State Key Program of National Natural Science Foundation (No. 50934003), National Natural Science Foundation of China (No. 11372033) for financial support.

Reference

[1] Dehyadegari E and Rabbani A R 2014 *Petrol Sci Technol* **32(23)** 2853-2866
[2] Liao X, Zhao H 2014 The Evaluation of CO2 Miscible Displacement and Storage Effect in Mature Oil Fields [J] *Petrol Sci Technol* **32(1)** 8-14
[3] Han L, Gu Y 2014 *Energy & Fuels* **28(11)** 6811-6819
[4] Hou Jian,Zhang Shunkang,Yuan Shibao 2006 *Water dynamics research and progress in A series* **21 (1)** 41-45
[5] Zhu Huayin, Zhou Juan,Wan Yujin 2004 *Geological oil experiment* **26 (6)** 571-573
[6] Feng Qingxian,Tang Guoqing,Chen Zhiyu,et al. 1995 *J Oil Gas Recov T* **2 (4)** 6-13
[7] Li Y, Li J, Ding S and Sun X 2014 *J. Dispersion Sci. Technol* **35(7)** 898-906
[8] Jafari S, Khezrnejad A, Shahrokhi O, et al. 2015.*Int J Oil Gas Coal T* **9(2)** 169-179
[9] Motealleh M, Kharrat R and Hashemi A 2013 An. *Energ Source Part A.* **35(13)** 1187-1196